

Preclinical Evaluation of a Novel ATM Inhibitor, KU59403, *In Vitro* and *In Vivo* in p53 Functional and Dysfunctional Models of Human Cancer

Michael A. Batey¹, Yan Zhao¹, Suzanne Kyle¹, Caroline Richardson², Andrew Slade², Niall M.B. Martin², Alan Lau², David R. Newell², and Nicola J. Curtin¹

Abstract

Ataxia telangiectasia mutated (ATM) kinase signals DNA double-strand breaks (DSB) to cell-cycle arrest via p53 and DNA repair. ATM-defective cells are sensitive to DSB-inducing agents, making ATM an attractive target for anticancer chemo- and radiosensitization. KU59403 is an ATM inhibitor with the potency, selectivity, and solubility for advanced preclinical evaluation. KU59403 was not cytotoxic to human cancer cell lines (SW620, LoVo, HCT116, and MDA-MB-231) *per se* but significantly increased the cytotoxicity of topoisomerase I and II poisons: camptothecin, etoposide, and doxorubicin. Chemo- and radiosensitization by ATM inhibition was not p53-dependent. Following administration to mice, KU59403 distributed to tissues and concentrations exceeding those required for *in vitro* activity were maintained for at least 4 hours in tumor xenografts. KU59403 significantly enhanced the antitumor activity of topoisomerase poisons in mice bearing human colon cancer xenografts (SW620 and HCT116) at doses that were nontoxic alone and well-tolerated in combination. Chemosensitization was both dose- and schedule-dependent. KU59403 represents a major advance in ATM inhibitor development, being the first compound to show good tissue distribution and significant chemosensitization in *in vivo* models of human cancer, without major toxicity. KU59403 provides the first proof-of-principle preclinical data to support the future clinical development of ATM inhibitors. *Mol Cancer Ther*; 12(6); 959–67. ©2013 AACR.

Introduction

DNA is constantly being damaged either from endogenous sources or environmental mutagens and carcinogens. DNA double-strand breaks (DSB) are particularly cytotoxic and cells mount a coordinated response of cell-cycle arrest and DNA repair in response to these lesions (1). The Ataxia Telangiectasia Mutated (ATM) kinase is a major coordinator of the DSB response and is the product of the *ATM* gene, which is defective in the disease Ataxia Telangiectasia (A-T) that is characterized by neurodegeneration, immunodeficiency, cancer predisposition, and an extreme hypersensitivity to ionizing radiation (IR) and other DSB-inducing agents (2). In response to DSBs, ATM initiates a cascade of phosphorylation events to induce

cell-cycle arrest via p53 and other checkpoint proteins (reviewed in ref. 3) and promote DNA repair by both homologous recombination and nonhomologous end-joining (4, 5).

IR and topoisomerase poisons are important anticancer agents that induce DNA DSBs. It is estimated that 1 Gy of irradiation induces 1,000 single-strand breaks and 25 to 40 double-strand DNA breaks per diploid cell (6). Topoisomerase II poisons, by stabilizing the topoisomerase II–DNA cleavable complex, cause persistent protein-associated DNA DSBs, whereas topoisomerase I poisons stabilize the topoisomerase I–DNA cleavable complex to cause persistent single-strand breaks that are converted to DSB at replication. A-T cells display defective p53 induction and loss of cell-cycle arrest; however, lack of ATM also confers radiosensitivity in some p53-null mouse tissues suggesting the existence of a p53-independent ATM effector pathway (7). ATM inhibition is therefore an attractive approach to anticancer chemo- and radiosensitization (8) with potential benefits in both p53 functional and dysfunctional cancers.

The C-terminal domain of ATM contains the serine threonine kinase signature motif characteristic of the phosphoinositide 3-kinase (PI3K) family (9). The PI3K inhibitor LY294002 (Table 1) inhibits other members of the PI3K family (10), and we previously used scaffold hopping from LY294002 to develop KU55933 as a selective

Authors' Affiliations: ¹Newcastle University, Newcastle Cancer Centre, Northern Institute for Cancer Research, Medical School, Newcastle upon Tyne; and ²KuDOS Pharmaceuticals, Ltd., Cambridge, United Kingdom

Note: Supplementary data for this article are available at Molecular Cancer Therapeutics Online (<http://mct.aacrjournals.org>).

Corresponding Author: Nicola J. Curtin, Newcastle University, Newcastle Cancer Centre, Northern Institute for Cancer Research, Medical School, Framlington Place, Newcastle upon Tyne, NE2 4HH, United Kingdom. Phone: 440-191-2464415; Fax: 440-191-2464301; E-mail: n.j.curtin@ncl.ac.uk

doi: 10.1158/1535-7163.MCT-12-0707

©2013 American Association for Cancer Research.

confirmed to be free of mycoplasma contamination and LoVo, SW620, HCT116, and MDA-MB-231 were authenticated by short tandem repeat (STR) profiling (LGC Standards). The population doubling time of the cells was approximately 24 hours.

Cytotoxicity and growth inhibition studies

We determined the effect of KU55933 and KU59403 on cellular survival following exposure to X-ray irradiation or the topoisomerase II poisons, etoposide and doxorubicin, and the topoisomerase I poison, camptothecin (Supplementary Fig. S2) by clonogenic assay as described previously (15). Briefly, exponentially growing cells were exposed to the cytotoxic agent with or without KU55933 (10 $\mu\text{mol/L}$) or KU59403 (1.0 $\mu\text{mol/L}$) for 16 hours, and survival was calculated by comparison to the appropriate control (0.5% DMSO or ATM inhibitor alone). The dose modification ratio was calculated as the percentage surviving cells (compared with control) treated with the cytotoxic agent alone, divided by the percentage surviving cells treated with the cytotoxic agent and the ATM inhibitor.

KU55933 and KU59403 pharmacokinetic and tissue distribution studies

All *in vivo* experiments were reviewed and approved by the relevant institutional animal welfare committees and carried out according to national law and published guidelines (16). SW620 colorectal tumor cells (1×10^7 cells in 50 μL culture medium per animal) were injected subcutaneously into the flanks of female athymic nude mice (CD1 *nu/nu*, Charles River), and tissue distribution studies were conducted when tumors had reached a size of approximately 650 mm^3 . KU59403 was given at 25 mg/kg to non-tumor-bearing female Balb/C mice or 50 mg/kg to SW620 tumor-bearing female nude mice. For comparison, KU55933 was administered at 10 mg/kg, which was the maximum administrable dose due to the limited solubility of KU55933 (i.e., 1 mg/mL even with the addition of 5% (v/v) DMSO and 10% (w/v) encapsin), to SW620-bearing nude mice. All doses were given at a dosing volume of 10 mL/kg via the intraperitoneal (i.p.) or intravenous route. Mice were bled under terminal anesthesia via cardiac puncture and the plasma fraction was stored at -20°C . Tissues were snap-frozen in liquid nitrogen and stored at -80°C until homogenization in PBS (1:3 w/v), using a stirrer macerator homogenizer (Werke GmbH & Co.) immediately before assay.

HPLC analysis of ATM inhibitors in plasma and tissue homogenates

KU55933 and KU59403 were extracted from plasma and tissue homogenates (50 μL) and analyzed by high-performance liquid chromatography (HPLC) as described previously (15). Plasma samples were quantified using a standard curve, prepared in plasma that was linear over the range: 0.05–10 $\mu\text{g/mL}$ ($r^2 > 0.9$) with duplicate QA standards (at 0.1, 1, and 10 $\mu\text{g/mL}$). Tissue concentrations

were calculated using the method of addition (17) to account for the efficiency of recovery and compensate for intersample variation.

Antitumor efficacy studies

CD-1 nude mice were implanted with SW620 or HCT116-N7 human cancer cell lines at 1×10^7 cells per animal s.c. ($n = 5$ per group). Treatment began when tumors were palpable ($\sim 5 \times 5 \text{ mm}^2$, 8–10 days postimplantation) with normal saline (control animals), KU59403 as indicated in the Results section, alone or in combination with etoposide phosphate or irinotecan (CPT-11). For combinations, the first daily dose of KU59403 was administered immediately before etoposide phosphate or irinotecan unless otherwise indicated. Tumor volume was calculated from 2-dimensional electronic caliper (Mitutoyo) measurements using the equation $a^2 \times b/2$ where a is the smallest measurement and b the largest. Data are presented as the median relative tumor volume (RTV), where the tumor volume for each animal on the initial day of treatment (day 0) is assigned an RTV value of 1.

Statistical analysis

Data were analyzed using GraphPad Prism software (GraphPad Software, Inc.). For the *in vitro* studies, significant differences between the effect of cytotoxic agent alone and cytotoxic agent plus KU59403 were determined by the Student *t* test (parametric). For *in vivo* studies, significant differences between the time take to reach RTV were determined by Mann–Whitney test.

Results

In vitro activity of KU59403 and p53 independence of chemo- and radiosensitization

KU59403 is a novel ATM inhibitor developed from LY294002 (Table 1), which is more potent against ATM than the previous lead KU55933 ($\text{IC}_{50} = 3$ vs. 13 nmol/L) and has at least 1,000 times greater specificity for ATM over other members of the PI3K family tested.

In contrast to the concentrations of 10 $\mu\text{mol/L}$ of KU55933 and 3 $\mu\text{mol/L}$ KU600019 needed to induce *in vitro* chemo- and radiosensitization (11, 12), KU59403 was an effective chemosensitizer at a concentration of 1 $\mu\text{mol/L}$. At this concentration, KU59403 inhibited ATM activity in SW620 cells by more than 50% and at the higher concentration of 10 $\mu\text{mol/L}$, KU55933 also substantially inhibited ATM activity (Supplementary Fig. S3). KU59403 alone was not significantly cytotoxic to LoVo or SW620 cells ($88\% \pm 7\%$ and $91\% \pm 6\%$ survival, respectively) but it enhanced camptothecin cytotoxicity (Fig. 1A, Table 2) in both cell lines with greater enhancement being observed in the LoVo than in the SW620 cells (7-fold; $P = 0.038$ vs. 4-fold; $P = 0.014$ at 10 nmol/L camptothecin). KU59403 also significantly enhanced the cytotoxicity of fixed concentrations of etoposide (0.1 and 1 $\mu\text{mol/L}$) or doxorubicin (10 or 100 nmol/L) in these cell lines, with greater enhancement of etoposide in SW620 cells and of doxorubicin in LoVo cells (Table 2).

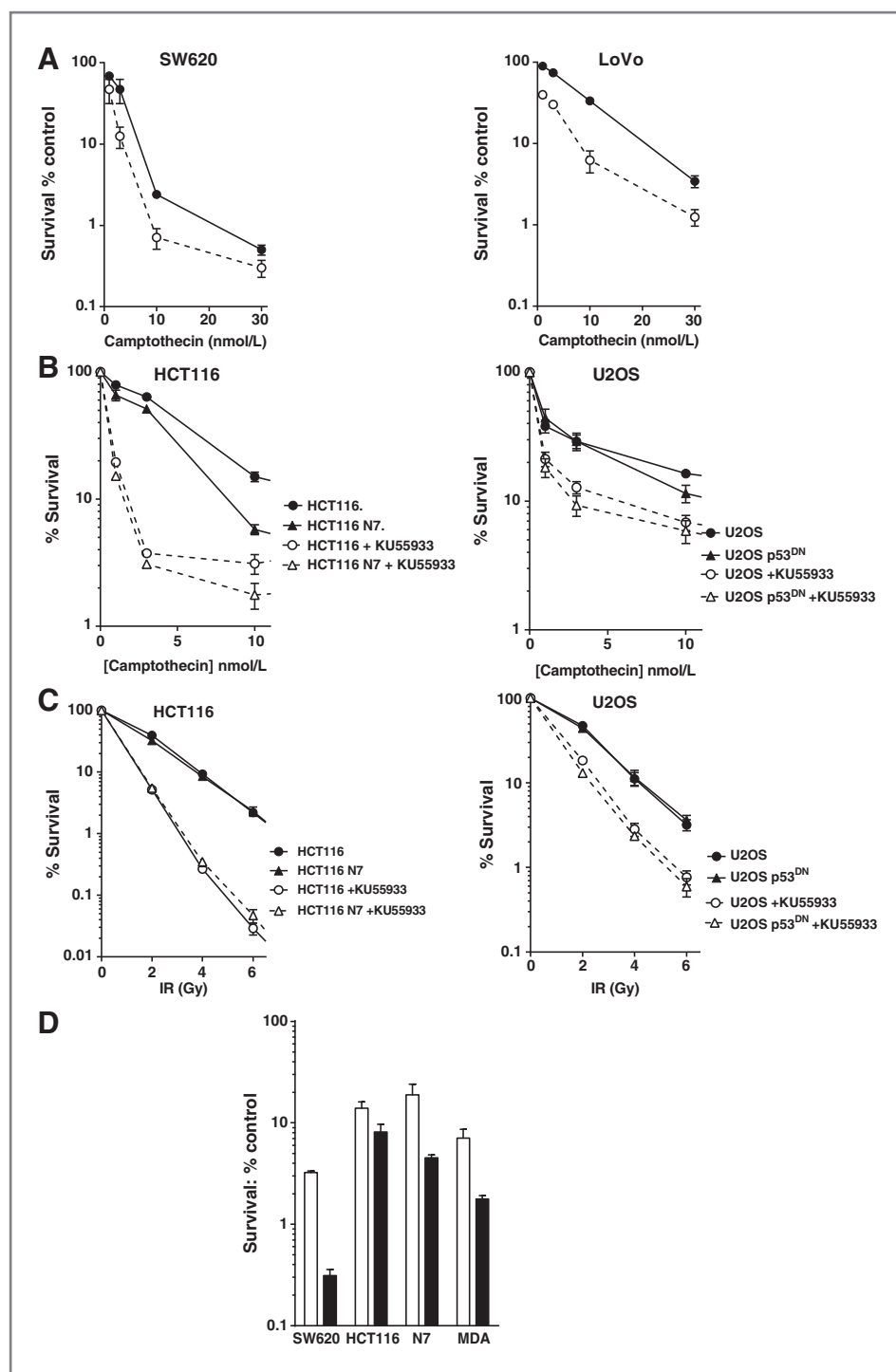


Figure 1. *In vitro* chemosensitization. A, sensitization of SW620 (left) and LoVo cells (right) to camptothecin by KU59403. Cells were exposed to varying concentrations of camptothecin alone (filled circles, solid line) or in the presence of 1 $\mu\text{mol/L}$ KU59403 (open circles, dashed line) for 16 hours before seeding for colony formation. Data, normalized to DMSO or KU59403 alone control, are mean \pm SD from 3 independent experiments. B, survival of wt (circles) and p53 dysfunctional (triangles) HCT116 (left) and U2OS cells (right) following exposure to increasing concentrations of camptothecin in the presence (open symbols, dashed lines) or absence of KU59403 (filled symbols, solid line). Data, normalized to DMSO or KU59403 alone, are mean \pm SD from 3 independent experiments. C, survival of wt (circles) and p53 dysfunctional (triangles) HCT116 (left) and U2OS cells (right) to increasing doses of X-rays in the presence (open symbols, dashed lines) or absence of KU59403 (filled symbols, solid line). Data, normalized to DMSO or KU59403 alone, are mean \pm SD from 3 independent experiments. D, sensitization of SW620, HCT116, HCT116-N7, and MDA-MB-231 cells to etoposide by KU59403. Data are 1 $\mu\text{mol/L}$ etoposide alone (white bars) or 1 $\mu\text{mol/L}$ etoposide plus 1 $\mu\text{mol/L}$ KU59403 (black bars) mean \pm SD from 3 independent experiments.

There was no consistent difference in the enhancement of cytotoxicity in LoVo cells (wild-type p53) compared with SW620 cells (mutant p53) but as these cells were derived from different tumors, they could harbor other genotypic or phenotypic differences that might mask the effect of p53 status. For this reason, we investigated whether chemo- and radiosensitivity was enhanced by ATM inhibition in a p53-dependent manner using paired

cell lines with functional or dysfunctional p53 using KU59403 as a model compound to confirm the data with KU59403 in proof of principle studies. KU59403 (10 $\mu\text{mol/L}$) sensitized p53 functional and dysfunctional HCT116 and U2OS cells to camptothecin to a similar extent (4- to 5-fold, Fig. 1B and Supplementary Table S1). Radiosensitization by KU59403 was greater in HCT116 than in U2OS cells but the p53 status did not

Table 2. Cytotoxicity of etoposide, doxorubicin, and camptothecin, alone and in combination with KU59403 in LoVo and SW620 cells

Cytotoxic drug	SW620			LoVo		
	% Survival			% Survival		
	Cytotoxic alone	Cytotoxic + KU59403	Enhancement factor ^a	Cytotoxic alone	Cytotoxic + KU59403	Enhancement factor
Etoposide, 100 nmol/L	89 ± 8.3	35 ± 12 ^b	2.9 ± 1.5	58 ± 8.3	18 ± 0.5 ^b	3.3 ± 0.4
Etoposide, 1 μmol/L	3.8 ± 1.1	0.41 ± 0.23 ^c	12 ± 7	3.9 ± 0.8	1.1 ± 0.2 ^c	3.8 ± 1.5
Doxorubicin, 10 nmol/L	50 ± 9	17 ± 0.2 ^c	2.9 ± 0.6	47 ± 3.1	16 ± 6.9 ^c	3.2 ± 1
Doxorubicin, 100 nmol/L	0.02 ± 0.01	0.01 ± .001	1.8 ± 0.7	2.1 ± 0.5	0.35 ± 0.04 ^c	6.1 ± 2.1
Camptothecin, 10 nmol/L	2.4 ± 0.2	0.71 ± 0.35 ^c	4.3 ± 2.8	33 ± 7.9	6.2 ± 3.8 ^c	6.9 ± 3.8

NOTE: Cells were exposed to etoposide or doxorubicin, at the concentrations indicated, alone or in combination with 1 μmol/L KU59403 in a final concentration of 0.5% (v/v) DMSO for 16 hours. Data, normalized in comparison with DMSO or KU59403 alone control, as appropriate, are the mean ± SD of 3 independent experiments.

^aEnhancement factor is defined as the survival with the cytotoxic alone/survival with cytotoxic + KU59403 in each individual experiment, and data are the mean ± SD of 3 independent experiments.

^bSignificant differences between cytotoxic drug alone versus cytotoxic + KU59404 is given by $P < 0.01$.

^cSignificant differences between cytotoxic drug alone versus cytotoxic + KU59404 is given by $P < 0.05$.

affect radiosensitivity or enhancement by KU55933 (Fig. 1C and Supplementary Table S1). The p53 status of the cell did not have a consistent effect on chemosensitization of topoisomerase II poisons by KU55933 either, for example, p53 dysfunction conferred reduced sensitization to etoposide and doxorubicin in U2OS cells but had no significant impact in HCT116 cells (Supplementary Table S2). Consistent with the p53 independence of chemo- and radiosensitization, KU55933 increased the G₂ cell-cycle arrest induced by IR, camptothecin, doxorubicin, and etoposide to a similar extent in p53 functional and dysfunctional cells and did not affect DNA DSB formation or repair kinetics (Supplementary Figs. S4 and S5). These data were confirmed with KU59403 (1 μmol/L), which enhanced etoposide (1 μmol/L) cytotoxicity to a similar extent in HCT116 and HCT116-N7 cells by 2.3 ± 1.6-fold ($P = 0.011$) and 3.8 ± 2.5-fold ($P = 0.019$), respectively, and in the p53-mutant SW620 cells and human breast cancer cell line, MDA-MB-231, sensitization was 11.9 ± 4.7 ($P < 0.0001$) and 3.8 ± 1.8-fold ($P = 0.006$), respectively (Fig. 1D). Inhibition of IR-induced ATM activity by KU59403 (1 μmol/L) was approximately 50% in MDA-MB231 cells and more than 50% in HCT116 cells that have low ATM expression and activity (Supplementary Fig. S3). These data indicate that p53 status has no major impact on sensitization by KU59403 and that SW620 cells, where a 12-fold enhancement was observed, are the most susceptible to etoposide sensitization by ATM inhibition. On the basis of these data, SW620 tumors treated with etoposide were chosen as our primary model system for the evaluation of KU59403 in *in vivo* studies.

Pharmacokinetics

As part of initial studies, plasma and tumor concentrations of drug were measured at 1 and 4 hours after

administration of a single dose of KU59403 at 50 mg/kg i.p. and KU55933 at the maximum administrable dose of 10 mg/kg. The plasma concentration of KU59403 was 5 μmol/L and maintained for at least 4 hours. In comparison, plasma levels of KU55933 were just over 1 μmol/L, consistent with the 5-fold lower dose administered (Fig. 2A). KU59403 accumulated in tumor tissue up to the 4-hour time point with a concentration at this time of 1.9 μmol/L, which is greater than that shown to be necessary for activity in the *in vitro* studies (Fig. 2A). In contrast, the levels of KU55933 in the tumor were below the limit of detection (0.5 μmol/L). To determine the pharmacokinetics of KU59403 in normal tissues, the compound was administered to female Balb/C mice at 25 mg/kg intravenously (Fig. 2B). In contrast to the previous experiment, KU59403 was cleared rapidly from the plasma, and at 4 hours, the plasma concentration was less than 0.1 μmol/L. This difference could be due to different route of administration, different dose- or strain-specific metabolism. There was, nevertheless, substantial accumulation and retention in the tissues, especially the liver, indicating that hepatic clearance may be the main route of elimination of this compound. At this dose and route of administration, KU59403 achieved concentrations in tissues in excess of those required for *in vitro* chemosensitization.

Antitumor efficacy studies

To investigate whether the marked chemosensitization by KU59403 observed *in vitro* could be reproduced *in vivo*, we treated mice bearing SW620 tumor xenografts with etoposide phosphate (etopophos) at a fixed dose of 11.35 mg/kg (equivalent to 10 mg/kg free etoposide) i.p. daily for 5 days or irinotecan (2.5 mg/kg i.p.) daily for 5 days alone and in combination with KU59403. We also investigated the dose and schedule dependency of KU59403

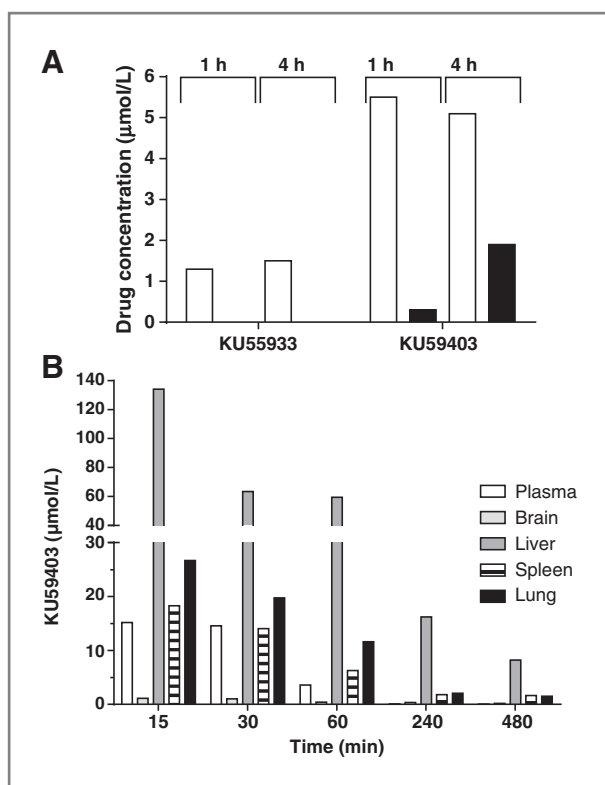


Figure 2. Tissue distribution of KU59403. A, plasma (white bars) and tumor (black bars) concentrations 1 and 4 hours after i.p. administration of KU59403 (50 mg/kg) or KU55933 (10 mg/kg) to female CD-1 athymic mice bearing the SW620 tumor xenograft subcutaneously. B, tissue concentrations of KU59403 following treatment of Balb/C mice with 25 mg/kg KU59403 i.v. Concentrations of KU59403 were determined in plasma (white bars) and tissue homogenates (brain, pale gray bars; liver, dark gray bars; spleen, striped bars; lung, black bars) by HPLC at various time points postadministration as indicated. Data are the mean of 3 samples from 3 mice per time point from a single experiment.

administration in combination with etopophos. KU59403 was given at doses of 6, 12.5, and 25 mg/kg i.p. twice daily (0 and 4 hours) and 12.5 mg/kg once daily, either immediately before etopophos dosing or 4 hours after etopophos dosing.

Tumors in control mice reached 4 times their starting volume (RTV4) at a median time of 6.5 days (Fig. 3A, Table 3). Treatment with etopophos alone caused a modest tumor growth delay of 4 days (time to RTV4 = 10.5 days). This delay was extended to 8.5 days (time to RTV4 = 15 days, $p = 0.093$) when given with KU59403 at 12.5 mg/kg i.p. twice daily for 5 days and 11.5 days (time to RTV4 = 18 days) when given with KU59403 at 25 mg/kg i.p. twice daily for 5 days. This latter treatment was the most effective dosing schedule for KU59403 identified; increasing etopophos efficacy by 190% ($P = 0.032$; Table 3). In contrast, when KU59403 was administered 4 hours after etopophos administration, there was no increase in efficacy compared with etopophos alone. In the above studies, neither KU59403 nor etopophos given as a single agent caused any measurable toxicity (maximum body weight

loss < 2%) and the combination of drugs did not cause unacceptable toxicity (maximum body weight loss = 7%; Supplementary Fig. S5A).

To investigate the enhancement of etopophos by KU59403 in a different xenograft model, mice bearing HCT116-N7 tumors were treated with vehicle alone, etopophos 11.35 mg/kg i.p. daily for 5 days, and/or KU59403 25 mg/kg i.p. twice daily for 5 days (Supplementary Fig. S4B). These tumors grew rapidly with tumors reaching RTV4 at 4.5 days, and HCT116-N7 tumors were resistant to etopophos alone (median time to RTV4 = 5.5 days). However, the etopophos-induced tumor growth delay was extended to 8.5 days by co-administration of KU59403, representing a 300% enhancement of etopophos activity that was statistically significant (Mann-Whitney test, $P = 0.037$). Toxicity, as measured by body weight loss, was tolerable and transient (Supplementary Fig. S5B).

Irinotecan, a member of the camptothecin group of compounds, is commonly used in the treatment of colon cancer. In this study, irinotecan alone caused an initial modest regression of the SW620 tumor followed by rapid regrowth resulting in a tumor growth delay of 7.5 days, which was extended to 19.5 days by the co-administration of KU59403. This represents a 144% enhancement of irinotecan-induced tumor growth delay, which was significantly different from irinotecan alone ($P = 0.032$; Fig. 3C, Table 3). There were no unacceptable adverse effects on animal body weights at any of the doses given in this study (Supplementary Fig. S5C). As is clearly indicated from these data, enhancement of the efficacy of etopophos can be obtained in the SW620 and HCT116 xenograft models, and of irinotecan in the SW620 model, by combination with KU59403 with little enhancement of toxicity (measured by body weight loss).

Discussion

We had previously identified KU55933 as a potent and selective inhibitor of ATM (11), and subsequently KU600019 has been identified as a more potent ATM inhibitor (12). Unfortunately, although these compounds provided *in vitro* evidence that inhibiting ATM induced chemo- and radiosensitization in tumor cell lines, to date, there have been no *in vivo* investigations with small-molecule ATM inhibitors. Here, we described KU59403, a novel inhibitor of the ATM kinase that is more potent ($IC_{50} = 3$ nmol/L) and specific (at least 1,000-fold selective for ATM compared with the other members of the PIKK family tested) than previously described compounds of this class. As well as improved potency over KU55933, KU59403 also exhibits improved solubility, enabling us to determine the effect of ATM inhibition in animal models of human cancer for the first time.

KU59403 had no inherent cytotoxicity *in vitro* at a concentration (1 µmol/L) sufficient to cause marked chemopotentialization of topoisomerase I and II poisons, making it the most potent ATM inhibitor described to date.

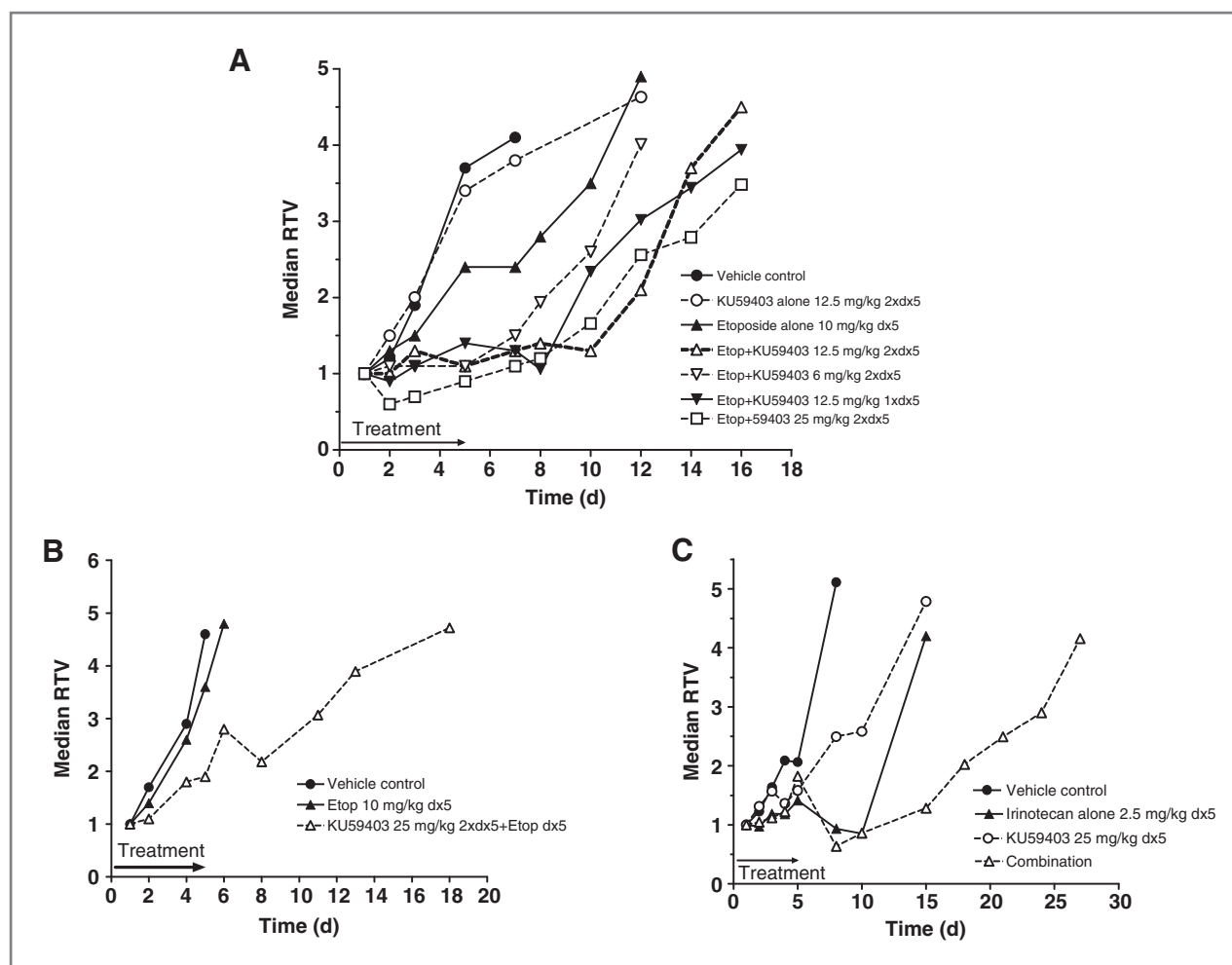


Figure 3. Antitumor efficacy of KU59403 in combination with topoisomerase poisons. **A**, SW620 xenograft: KU59403 in combination with etoposide phosphate. CD-1 nude mice were treated with vehicle control (filled circles, solid line), KU59403 12.5 mg/kg 2 × daily × 5 (open circles, dashed line), etoposide phosphate 10 mg/kg daily × 5 alone (filled triangles, solid line) or in combination with KU59403 12.5 mg/kg 2 × daily × 5 (open triangles, dashed line), KU59403 6 mg/kg 2 × daily × 5 (open inverted triangles, dashed line), KU59403 12.5 mg/kg 1 × daily × 5 (filled inverted triangles, solid line), or KU59403 25 mg/kg 2 × daily × 5 (open squares, dashed line). Growth of SW620 xenografts is presented as the median RTV of groups of 5 animals. **B**, HCT116 N7 xenograft: KU59403 in combination with etoposide phosphate. CD-1 nude mice were treated with vehicle control (filled circles, solid line), etoposide phosphate 10 mg/kg daily × 5 alone (filled triangles, solid line) or in combination with KU59403 25 mg/kg 2 × daily × 5 (open triangles, dashed line). Growth of HCT116-N7 xenografts is presented as the median RTV of groups of 5 animals. **C**, SW620 xenograft: KU59403 in combination with irinotecan. CD-1 nude mice were treated with vehicle control (filled circles, solid line), KU59403 12.5 mg/kg 2 × daily × 5 (open circles, dashed line), irinotecan 2.5 mg/kg daily × 5 alone (filled triangles, solid line) or in combination with KU59403 25 mg/kg 2 × daily × 5 (open triangles, dashed line). Growth of SW620 xenografts is presented as the median RTV of groups of 5 animals.

Enhancement of etoposide cytotoxicity, ranging from 3- to 12-fold, was observed in a panel of human tumor cell lines with the greatest sensitization observed in SW620 cells. Interestingly, KU59403 only induced 2- to 3-fold sensitization of etoposide in HCT116 cells, which have been reported to have reduced ATM expression due to promoter methylation (18) and defects in MRE11 (19). Sensitization in MDA-MB-231 cells, which are reported to have mutated *ATM* (20) was also relatively modest. Both of these cell lines had reduced ATM activation by IR (~4-fold) in comparison to SW620 cells (6- to 7-fold). Studies in matched p53-proficient and -deficient cell lines showed that p53 status had no impact on chemosensitiza-

tion by KU59403 or KU55933, and p53 status was not a determinant of the effect of KU55933 on cell-cycle arrest or DNA DSB repair. Cytotoxic drug or IR exposure resulted in G₂ arrest in cells with both wild-type and dysfunctional p53 suggesting that G₁ checkpoints were compromised in these cells irrespective of p53 status (21). The G₂ arrest was enhanced by KU49403 independently of p53 status but whether this reflects further impairment of the G₁ checkpoint, or that ATR signaling to the G₂ checkpoint is increased when ATM is inhibited, remains to be determined.

Pharmacokinetic investigation of KU59403 revealed a more rapid clearance in Balb/C mice after an intravenous

Table 3. Chemosensitization of antitumor activity determined in mice bearing SW620 xenografts

Treatment	Nadir % starting body weight	Time to RTV4	Delay, ^a d	Enhancement (%) ^b
Vehicle control	96.3	6.5		
KU59403 12.5 mg/kg 2× daily × 5	100	7	0.5	
Etophos (equivalent to 10 mg/kg etoposide) daily × 5	98.6	10.5	4	
Etophos + KU59403 6 mg/kg 2× daily × 5	96.9	12	5.5	38
Etophos + KU59403 12.5 mg/kg 2× daily × 5	94.9	15	8.5	113 ^d
Etophos + KU59403 25 mg/kg 2× daily × 5	93.3	18	11.5	190 ^c
Etophos + KU59403 12.5 mg/kg 1× daily × 5 concurrent	96.5	16.5	10	150
Etophos + KU59403 12.5 mg/kg 1× daily × 5 h post	94.3	10	3.5	0
Irinotecan 2.5 mg/kg daily × 5	93.6	14.5	8	
KU59403 25 mg/kg daily × 5	99.7	12	5.5	
Irinotecan + KU59403 25 mg/kg daily × 5	100	26	19.5	144 ^c

^aDelay (days) is the tumor growth delay, which is calculated as the time to median relative tumor volume 4 (median RTV4) following relevant treatment minus time to median RTV4 in control mice.

^bEnhancement (%) is calculated as $[100 \times (\text{delay combination}/\text{delay cytotoxic alone})] - 100$.

^cIndicates statistically significant enhancement ($P < 0.05$).

^dIndicates marginally statistically significant enhancement ($P < 0.1$).

dose but that plasma concentrations were maintained for at least 4 hours in tumor-bearing CD1 nude mice after intraperitoneal administration. Whether this difference in clearance reflects the route of administration, dose or strain effects were not determined. The pharmacokinetic studies in tumor-bearing mice indicated that levels of KU59403 sufficient for chemosensitization *in vitro* could be maintained in the tumor for at least 4 hours. Although levels of KU59403 in excess of those required for chemo- and radiosensitization *in vitro* were also detected in normal tissues for at least 4 hours following a dose of 25 mg/kg i.p., which could potentially have toxic consequences. KU59403 was nontoxic alone and did not cause a profound increase in either etoposide or irinotecan toxicity.

Similar to the *in vitro* studies, KU59403 alone had no impact on tumor growth rate. However, it did enhance the antitumor activity of etoposide against SW620 xenografts in a dose- and schedule-dependent manner. Significant sensitization was seen with a single daily dose of KU59403 at 12.5 mg/kg; administration but splitting the same total dose into 2 separate injections of 6 mg/kg was not as effective. Increasing the dose of KU59403 to 25 mg/kg given twice daily resulted in the greatest chemosensitization with a 3-fold increase in etoposide-induced tumor growth delay in both SW620 and HCT116-N7 xenografts, in the absence of a significantly increased toxicity. This is in contrast to the *in vitro* data where KU59403 enhanced etoposide cytotoxicity to a greater extent (3- to 12-fold) in SW620 cells than HCT116-N7 cells (2- to 4-fold) and suggests that *in vitro* data do not entirely predict *in vivo* results. It is possible that the tumor microenvironment may influence the efficacy of the combination as we have previously observed with chemosensitization studies (22)

Interestingly, it would seem that it is necessary to have KU59403 present at the time of etoposide dosing to have an effect, as delaying the administration of KU59403 by only 4 hours completely abolished chemosensitization. As ATM signaling is proposed to be an early response to DNA DSB, these data confirm the need to inhibit ATM while DNA DSB are being induced.

We have also shown that KU59403 can be used to enhance the sensitivity of human colon cancer cell lines to topoisomerase I poisons both *in vitro* and *in vivo*. KU59403 was shown to enhance the activity of camptothecin in both SW620 and LoVo cells *in vitro* (4- and 7-fold, respectively) and gave a 144% enhancement of irinotecan efficacy in a SW620 human xenograft model. These data as a whole are very encouraging and support the further development of this class of compound.

In summary, our studies have shown that ATM is a valid target for the development of drugs designed to improve the activity of certain cytotoxic anticancer therapies. KU59403 is a potent and selective inhibitor of ATM, which is without intrinsic cytotoxicity but is a potent enhancer of topoisomerase I and II poison cytotoxicity *in vitro*. We have shown that KU59403 increases the efficacy of topoisomerase I and II poisons *in vivo* without intrinsic toxicity despite normal tissue exposure. These data provide further proof-of-principle evidence for the strategy of inhibiting ATM as a therapeutic maneuver for anticancer therapy.

Disclosure of Potential Conflicts of Interest

N.J. Curtin and D.R. Newell have received research funding from KuDOS Pharmaceuticals Ltd and AstraZeneca, the purchasers of KuDOS. A. Lau, N.M.B. Martin, C. Richardson, and A. Slade are former employees of KuDOS Pharmaceuticals. No potential conflicts of interest were disclosed by the other authors.

Authors' Contributions

Conception and design: M.A. Batey, Y. Zhao, N.M.B. Martin, D.R. Newell, N.J. Curtin

Development of methodology: M.A. Batey, Y. Zhao, C. Richardson
Acquisition of data (provided animals, acquired and managed patients, provided facilities, etc.): M.A. Batey, Y. Zhao, C. Richardson, N.M.B. Martin, A. Lau

Analysis and interpretation of data (e.g., statistical analysis, biostatistics, computational analysis): M.A. Batey, Y. Zhao, A. Slade, A. Lau, D.R. Newell, N.J. Curtin

Writing, review, and/or revision of the manuscript: M.A. Batey, A. Lau, D.R. Newell, N.J. Curtin

Administrative, technical, or material support (i.e., reporting or organizing data, constructing databases): M.A. Batey, Y. Zhao, S. Kyle, A. Slade

Study supervision: M.A. Batey, A. Slade, D.R. Newell, N.J. Curtin

Acknowledgments

The authors thank Graeme Smith for helpful discussions throughout the course of this work.

Grant Support

This work was supported by AstraZeneca and KuDOS Pharmaceuticals (grant number AZ305642 to N.J. Curtin and D.R. Newell) and Cancer Research UK (grant number C240/A7409 to D.R. Newell and N.J. Curtin).

The costs of publication of this article were defrayed in part by the payment of page charges. This article must therefore be hereby marked *advertisement* in accordance with 18 U.S.C. Section 1734 solely to indicate this fact.

Received July 9, 2012; revised February 4, 2013; accepted February 22, 2013; published OnlineFirst March 19, 2013.

References

- Kastan MB, Bartek J. Cell-cycle checkpoints and cancer. *Nature* 2004;432:316–23.
- Chun HH, Gatti RA. Ataxia Telangiectasia, an evolving phenotype. *DNA Repair (Amst)* 2004;3:1187–96.
- Shiloh Y. The ATM-mediated DNA damage response: taking shape. *TIBS* 2006;21:402–10.
- Cortez D, Wang Y, Qin J, Elledge SJ. Requirement of ATM-dependent phosphorylation of brca1 in the DNA damage response to double-strand breaks. *Science* 1999;286:1162–6.
- Riballo E, Kuhne M, Rief N, Doherty A, Smith GC, Recio MJ, et al. A pathway of double-strand break rejoining dependent upon ATM, Artemis, and proteins locating to gamma-H2AX foci. *Mol Cell* 2004; 16:715–24.
- Olive PL. The role of DNA single- and double-strand breaks in cell killing by ionising radiation. *Radiat Res* 1998;150:S42–S51.
- Westphal CH, Hoyes KP, Canman CE, Huang X, Kastan MB, Hendry JH, et al. Loss of ATM radiosensitizes multiple p53 null tissues. *Cancer Res* 1998;58:5637–9.
- Sarkaria JN, Eshleman JS. ATM as a target for novel radiosensitizers. *Semin Radiat Oncol* 2001;11:316–27.
- Durocher D, Jackson SP. DNA-PK, ATM and ATR as sensors of DNA damage: variations on a theme? *Curr Opin Cell Biol* 2001;13:225–31.
- Izzard RA, Jackson SP, Smith GCM. Competitive and non-competitive inhibition of the DNA dependent protein kinase. *Cancer Res* 1999;59: 2581–6.
- Hickson I, Zhao Y, Richardson CJ, Green SJ, Martin NMB, Orr AI, et al. Identification and characterization of a novel and specific inhibitor of the ataxia-telangiectasia mutated kinase ATM. *Cancer Res* 2004;64: 9152–9.
- Golding SE, Rosenberg E, Valerie N, Hussaini I, Frigerio M, Cockcroft XF, et al. Improved ATM kinase inhibitor KU-60019 radiosensitizes glioma cells, compromises insulin, AKT and ERK prosurvival signaling, and inhibits migration and invasion. *Mol Cancer Ther* 2009;8: 2894–902.
- Vikhanskaya F, Colella G, Valenti M, Parodi S, D'Incalci M, Brogginini M. Cooperation between p53 and hMLH1 in a human col carcinoma cell line in response to DNA damage. *Clin Cancer Res* 1999;5:937–41.
- Moumen A, Masterson P, O'Connor M, Jackson SJ. hnRNP K: An HDM2 target and transcriptional coactivator of p53 in response to DNA damage. *Cell* 2005;123:1065–78.
- Zhao Y, Thomas HD, Batey MA, Cowell IG, Richardson CJ, Griffin RJ, et al. Preclinical evaluation of a potent novel DNA-dependent protein kinase (DNA-PK) inhibitor, NU7441. *Cancer Res* 2006;66: 5354–62.
- Workman P, Aboagye EO, Balkwill F, Balmain A, Bruder G, Chaplin DJ, et al. Committee of the National Cancer Research Institute. Guidelines for the welfare and use of animals in cancer research. *Br J Cancer* 2010;102:1555–77.
- Potter GWH. Analysis of biological molecules: an introduction to principles, instrumentation and techniques. 1st ed. London, England: Chapman and Hall;1995.
- Kim WJ, Vo QN, Shrivastar M, Lataxes TA, Brown KD. Aberrant methylation of the ATM promoter correlates with increased radiosensitivity in human colorectal tumour cell line. *Oncogene* 2002;21:3864–71.
- Takemura H, Rao VA, Sordet O, Furuta T, Miao ZH, Meng L, et al. Defective Mre11-dependent activation of Chk2 by ataxia telangiectasia mutated in colorectal carcinoma cells in response to replication-dependent DNA double strand breaks. *J Biol Chem* 2006;281:30814–23.
- Lu Y, Condie A, Bennett JD, Fry MJ, Yuille MR, Shipley J. Disruption of the ATM gene in breast cancer. *Cancer Genet Cytogenet* 2001;126: 97–101.
- Massague J. G1 cell cycle control and cancer. *Nature* 2004;432: 298–306.
- Calabrese CR, Almassy R, Barton S, Batey MA, Calvert AH, Canan-Koch S, et al. Preclinical evaluation of a novel poly(ADP-ribose) polymerase-1 (PARP-1) inhibitor, AG14361, with significant anticancer chemo- and radio-sensitization activity. *J Natl Cancer Inst* 2004;96: 56–67.

Molecular Cancer Therapeutics

Preclinical Evaluation of a Novel ATM Inhibitor, KU59403, *In Vitro* and *In Vivo* in p53 Functional and Dysfunctional Models of Human Cancer

Michael A. Batey, Yan Zhao, Suzanne Kyle, et al.

Mol Cancer Ther 2013;12:959-967. Published OnlineFirst March 19, 2013.

Updated version Access the most recent version of this article at:
doi:[10.1158/1535-7163.MCT-12-0707](https://doi.org/10.1158/1535-7163.MCT-12-0707)

Cited articles This article cites 21 articles, 8 of which you can access for free at:
<http://mct.aacrjournals.org/content/12/6/959.full#ref-list-1>

Citing articles This article has been cited by 4 HighWire-hosted articles. Access the articles at:
<http://mct.aacrjournals.org/content/12/6/959.full#related-urls>

E-mail alerts [Sign up to receive free email-alerts](#) related to this article or journal.

Reprints and Subscriptions To order reprints of this article or to subscribe to the journal, contact the AACR Publications Department at pubs@aacr.org.

Permissions To request permission to re-use all or part of this article, use this link
<http://mct.aacrjournals.org/content/12/6/959>.
Click on "Request Permissions" which will take you to the Copyright Clearance Center's (CCC) Rightslink site.